

Numerical investigation of fully encased composite columns subjected to combined axial and cyclic loading

Almoutaz Bellah Alsamawi¹, Nadir Boumechra¹,

Karim Hamdaoui¹, Ebrahim Alkebsi² and Hamza Basri¹

¹ EOLE Research Laboratory, Department of Civil Engineering,
Faculty of Technology, University of Tlemcen, BP 230,
Tlemcen, Algeria.

² Laboratory of Mechanical structures and materials (LaMSM),
University of Batna 2, Batna, Algeria.

Abstract

This research investigated the cyclic behaviour of fully encased composite (FEC) columns. By constructing and investigating thirty-six FEC columns to increase the strength and performance of composite columns subjected to combined axial and cyclically increasing lateral loads. The goal of this research is to investigate the effect of the axial load ratio and concrete reinforcing bars on the behaviour of composite columns subjected to combined axial and cyclically increasing lateral loads. Finite element analysis was performed on each specimen, taking into account the inelastic behaviour of concrete, structural steel, and longitudinal and transverse steel bars. In this research, the finite element models created in ANSYS software were verified and calibrated against previously published experimental results. FEC columns are studied in terms of hysteretic performance, load-carrying capacity, energy dissipation capacity, ductility, and stiffness degradation. The composite columns provide an interesting result in the numerical simulation.

Keywords: cyclic loads fully encased composite columns, concrete reinforcement bars, axial load, and hysteretic curves.

1. Introduction

It's common to see composite columns in seismically or fire-prone areas because they provide the required rigidity to keep a building's lateral drift within acceptable limits and successfully resist lateral seismic and wind loads. A composite column will be able to resist a high load capacity while also providing economic benefits due to its reduced cross-section. By inserting steel into the centre of a cross-section column, it will be able to resist tensile loads, such as profile steel or reinforced steel and the column's ductility will improve. The combination of the two materials is predicted to be compatible since concrete has high compression strength and is also economical, while steel has high tensile strength, stiffness, and ductility. Concrete-encased column research on cyclic behaviour was somewhat limited and focused mostly on experimental studies of composite columns under cyclic lateral loads. Stirrup ratio and embedding depth ratio for steel-concrete composite columns were studied by Chen et al. (Chen et al., 2014). It was found that increasing the stirrup ratio improves seismic behaviour, that composite columns with cross-shaped steel perform better seismically than those with H-shaped steel, and that the minimal value of the embedded ratio of steel-concrete composite columns maybe 2.5. (Zhu et al., 2016) investigated the behaviour of steel reinforced high strength concrete columns (SRHC) under cyclic loading by testing the impacts of stirrup arrangement and structural steel details with studs. The SRHC columns with several stirrups had great deformation capacity and sufficient energy dissipation. Also, the studs had little effect on the performance of the SRHC columns during the early loading stage. Studs have a good influence on the seismic behaviour of SRHC columns after cover spilling.

Some previous researches have been also carried out on filled steel tube reinforced concrete columns (Gajalakshmi & Helena, 2012; Han, Huang, et al., 2009; Han, Liao, et al., 2009) and encased steel-concrete composite columns (A. B. Alsamawi et al., 2022; A. Alsamawi & Boumechra, 2021; Qian et al., 2016; Yue et al., 2019) under constant axial load and cyclic load, it was found that both columns exhibit favourable ductility and energy dissipation and are adaptable in areas with strong earthquakes. From the above works, it can be seen that investigations on the behaviour of composite columns are not yet sufficient, in order to completely understand the cyclic behaviour of composite columns, it is necessary to focus on the effects of the axial load ratio and the concrete reinforcement bars.

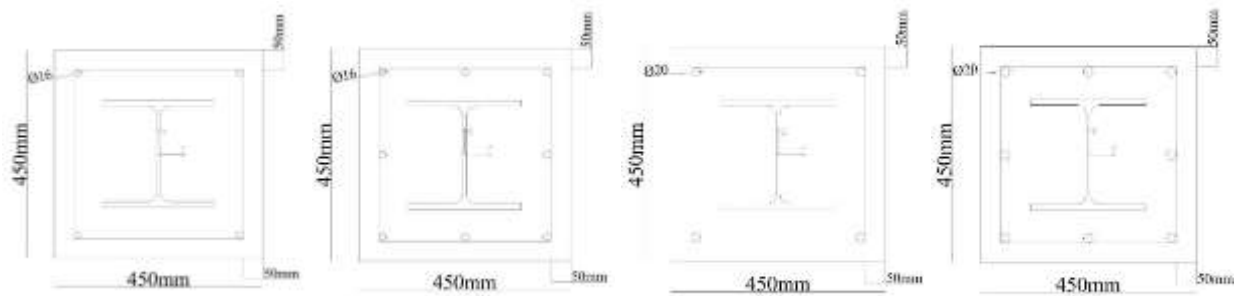
As a result, thirty-six designed specimens were numerically investigated under a combination of axial and cyclic loads using the ANSYS software's finite element analysis method. To evaluate the software's analysis results, the investigated model was first verified by comparing its results to previous experimental testing results conducted in labs by Aribert et al. (Aribert et al., 2003). The results of this verified analysis are included in previous work (A. B. Alsamawi et al., 2022). In addition to determining the columns' ultimate cyclic load capacity, energy dissipation, ductility, and stiffness were investigated. The purpose of this study is to investigate the axial load ratio and concrete reinforcing bars effects on FEC columns under cyclic loading.

1 Numerical modelling

1.1 Geometrical and Material Properties

The presence of reinforcement bars provides a beneficial residual strength following concrete crushing that leads to improved ductility. Four different percentages of longitudinal bars $4\phi 16$, $8\phi 16$, $4\phi 20$ and $8\phi 20$ (as shown in Figure 1) were used in the parametric study with 100mm, 150mm and 200mm of spacing between transversal bars as shown in Figure 2.

The cover concrete is 50 mm, the steel profile is HEA240 and the cross-section is 450x450 mm.



<i>Col</i>	<i>Col</i>	<i>Col</i>	<i>Col</i>
<i>um</i>	<i>um</i>	<i>um</i>	<i>um</i>
<i>ns</i>	<i>ns</i>	<i>ns</i>	<i>ns</i>
<i>of</i>	<i>of</i>	<i>of</i>	<i>of</i>
4φ	8φ	4φ	8φ
16	16.	20	20.

Figure 1: Dimensions of some designed composite columns.



Spacing of 100mm



Spacing of 150mm



Spacing of 200mm

Figure 2: FEC columns with different transversal bars.

In this numerical modelling, Poisson's ratio of steel is taken as 0.3 and modulus of elasticity as $E_s=210\ 000\ \text{Mpa}$, also the steel grade is S500 ($F_{sk}=500\ \text{Mpa}$), S275($F_y=275\ \text{Mpa}$) for reinforcing bars and steel section respectively, defined as elastic perfectly plastic as Figure 3. Poisson's ratio of concrete is taken as 0.2 and modulus of elasticity as $E_{cm}=31000\ \text{Mpa}$. The equivalent stress–strain relationship of concrete shown in Figure 3, proposed by Eurocode4 (Eurocode 4, 2004).

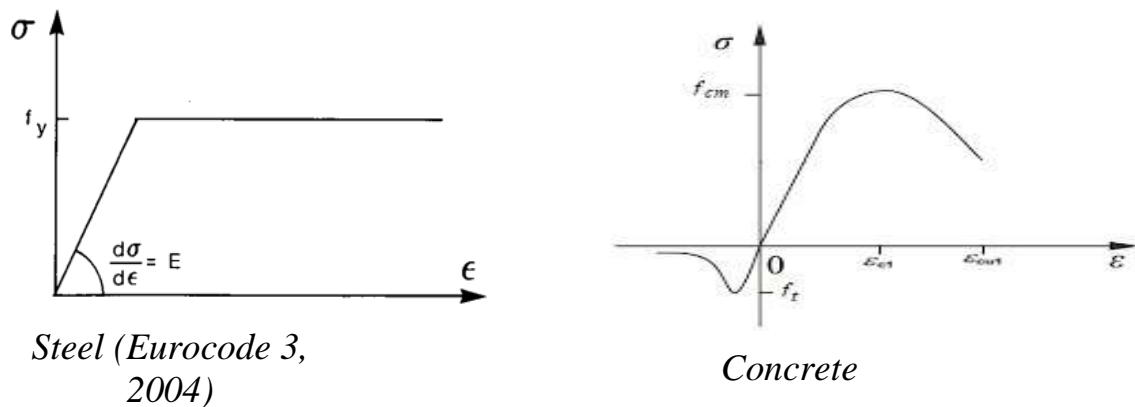


Figure 3: Bi-linear stress-strain relationship of materials (A. B. Alsamawi et al., 2022).

1.2 Finite element modelling and boundary conditions

Taking into account a number of prior research published in the literature (Alkebsi et al., 2021; A. Alsamawi & Boumechra, 2021). It was chosen to use the finite element models, Solid65 as concrete in 3-D solid modelling with reinforcing bars for its capability to crack in tension and crush in compression. The element is made up of eight nodes, each with three degrees of freedom. Steel section defined as Solid185 as in a three-dimensional model of solid structures with eight nodes each having three degrees of freedom. Plasticity, stress stiffening, big deflection, huge strain capacities, and creep also are properties of this element. The reinforcing bars, which are a uniaxial compression-tension element with three degrees of freedom at each node are specified as Link180.

The boundary conditions are fixed-free. To begin, an axial force was applied in the centre of the composite columns, and a horizontal load was applied with displacement utilising a boundary condition in various increments.

The columns were subjected to prescribed horizontal-displacement history under constant axial load calculated from the equation $P/N_{pb,Rk} = 0.1, 0.3$ and 0.5 with $N_{pb,Rk} = A_a \cdot F_y + 0.85 A_c \cdot F_{ck} + A_s \cdot F_{sk}$, according to Eurocode4 (Eurocode 4, 2004), these loads were applied at the top surface of the column.

1.3 Model validation

Two previously published test specimens by Aribert et al. (Aribert et al., 2003) were utilised for comparison to validate the accuracy of the numerical model for the composite columns described in the preceding section. The actual and calculated cyclic load (P) against lateral displacement (v) curves were compared in a previous study (A. B. Alsamawi et al., 2022). In general, there is good agreement between the numerical and tested curves.

2 Analysis of numerical results and discussion

The FE model built in this work was used to simulate and analyse the columns constructed for the parametric investigation (as presented in previous section). The parametric simulation for parametric columns also cyclic load against lateral displacement curves. To observe the effect of reinforcing bars, the stiffness, energy dissipation, and ductility were also determined.

2.1 Hysteresis Curves

The structures' load-lateral displacement curves contribute an important role in understanding inelastic behaviour and developing a seismic design methodology for these structures. Under completely reversed cyclic loading, the specimens draw the slip hysteresis loop. Figure 4 shows that the reinforcement bars effect has almost symmetrical hysteresis curves.

The hysteresis curves showed that the axial load has a significant impact on the FEC columns under cyclic loads, according to these series of simulations. Before the horizontal force reaches the yield load, the specimens behave almost elastically. From the yield load to the ultimate load, the specimens' rigidity gradually decreases, and plastic deformation is small. The specimens' hysteresis curves are strongly influenced by the axial compression ratio. The loops get bigger and more stable as the axial compression ratio decreases. The FEC columns are somewhat influenced by the transversal reinforcement bars. The FEC columns get stronger and stiffer as the spacing between transversal bars rises.

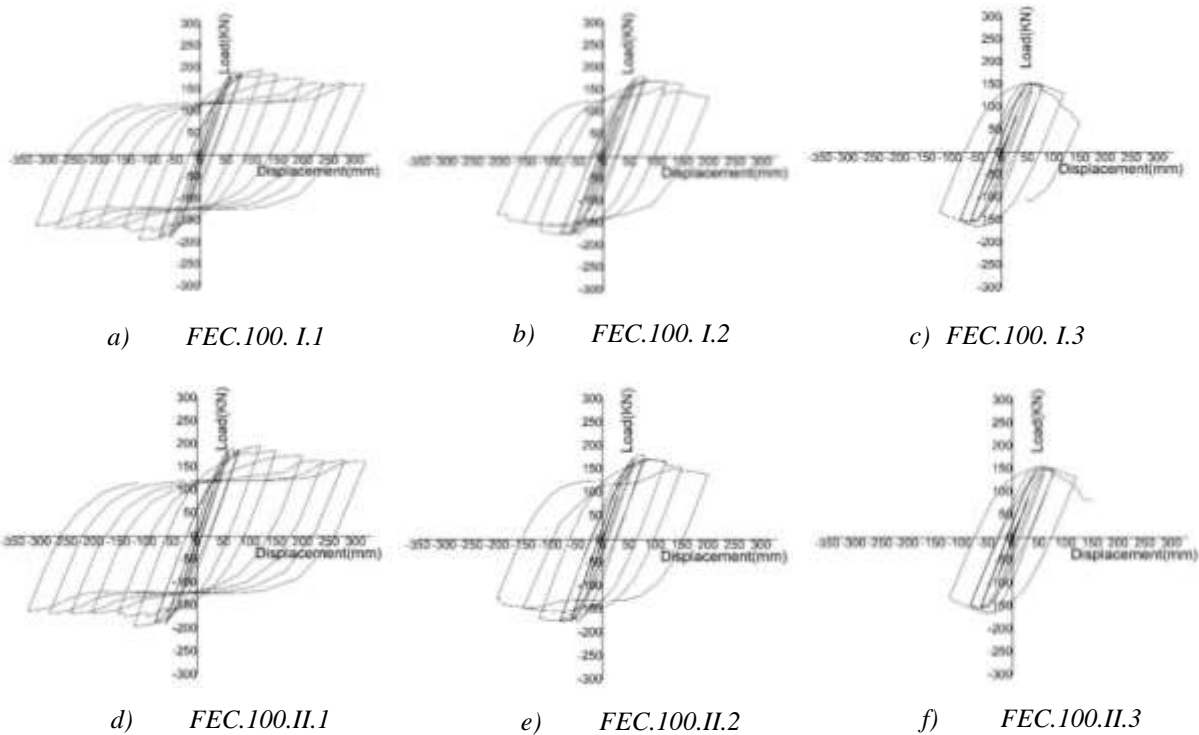
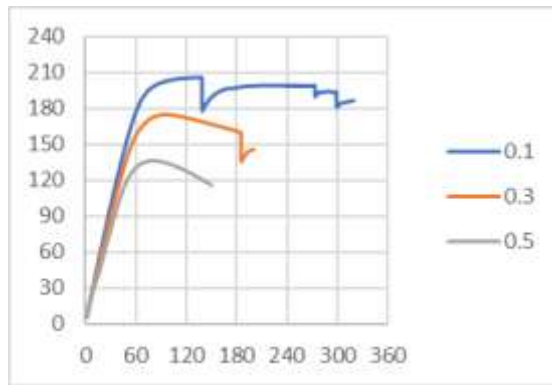


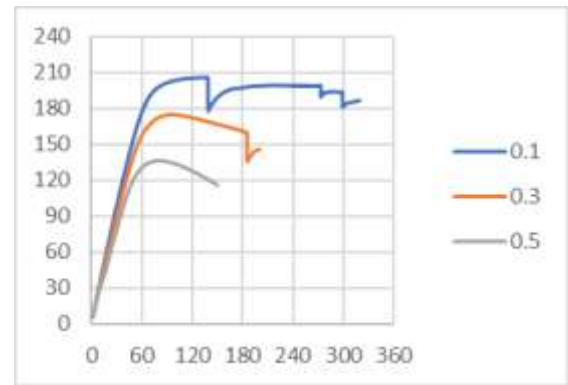
Figure 4: Some of hysteresis curves of the specimens.

2.2 Skeleton Curves

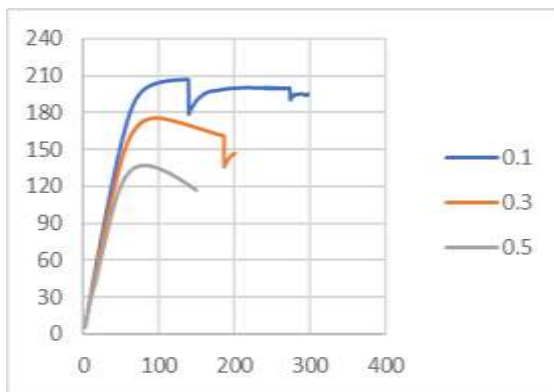
In order to create a skeleton curve, the peak points of each cycle's lateral load-displacement curves are connected. Figure 5 shows that specimens with a 0.5 ratio of axial load have the lowest peak load and initial stiffness, while the other two specimens show a 10.35%-27.73% increase in peak load, 50.31%-95.92% increase in initial stiffness and 13.74%-15.62% increase in ductility. It has been found that increasing the number of reinforcing bars has no effect on the peak load. This is because the load-bearing capacity of the steel section dominates the capacity of the reinforcing bars.



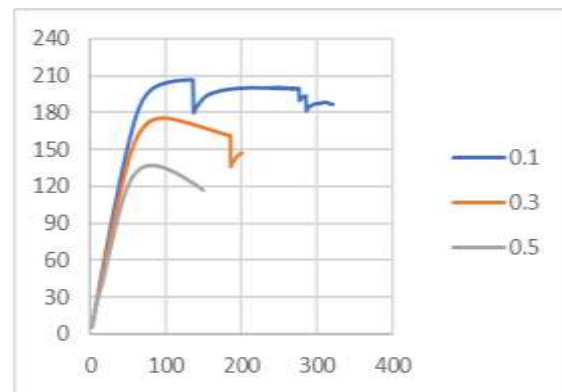
a) *FEC.100.I*



b) *FEC.100.II*



c) *FEC.100.III*



d) *FEC.100.IV*

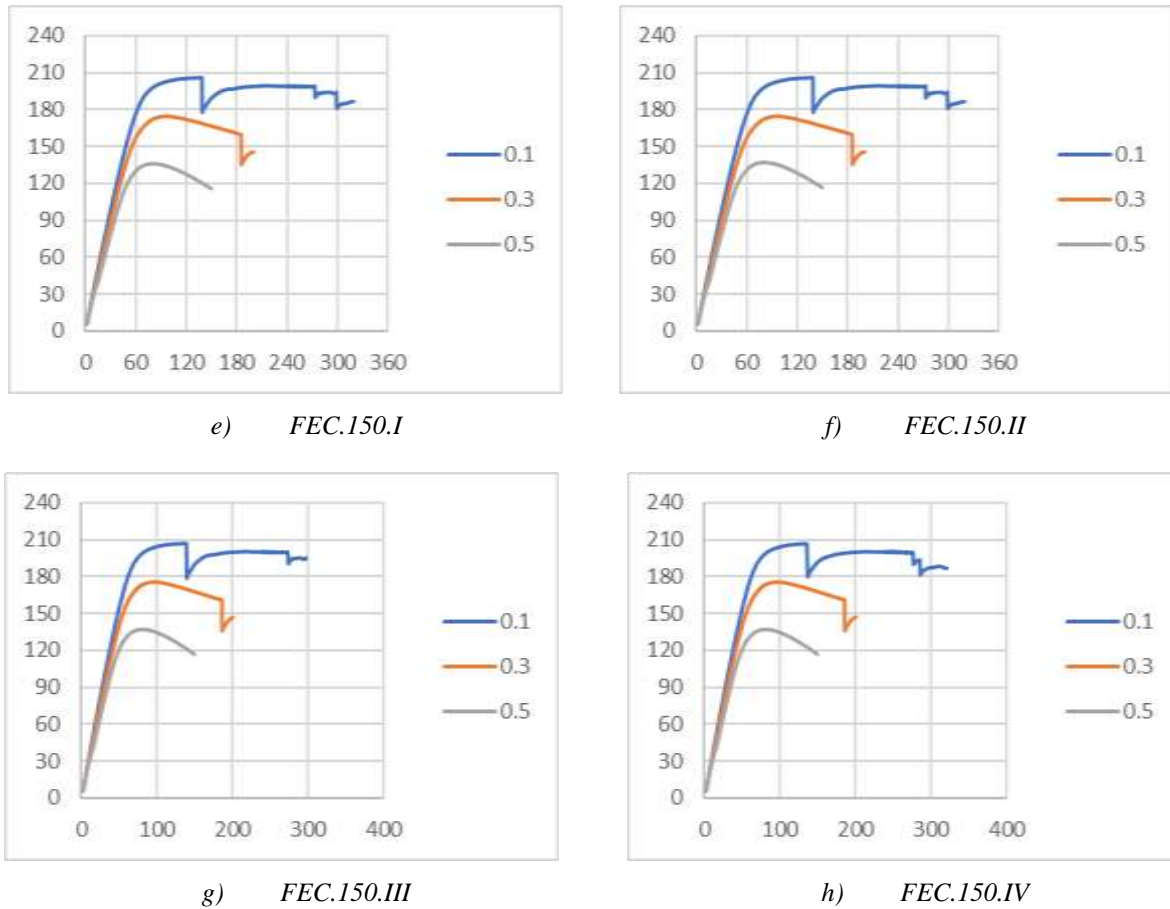


Figure 5: Comparison of skeleton curves.

2.3 Dissipated energy

An important factor in determining a structure's seismic performance is the amount of energy dissipated by each element. The area enclosed by the hysteretic hoops is estimated as dissipated energy from the lateral load-displacement curve (Campian et al., 2015). Figure 6 shows the outcomes of calculations. It can be seen that when the reinforcement bar ratio increases, the energy dissipation gradually increases. The energy dissipation capability of specimens with a 0.5 axial load ratio is the lowest. For specimens with $4\phi 16$, $8\phi 16$, $4\phi 20$ and $8\phi 20$, the plastic work done per cycles is similar. The dissipated energy for specimens with 0.1 axial load ratio and for $4\phi 16$, $8\phi 16$, $4\phi 20$ and $8\phi 20$ reinforcement bars is near 380KN.m, 382KN.m, 382KN.m and 384KN.m respectively.

Compared with the energy dissipation capacity of FEC columns with different spacing between transversal bars, it can be found that the specimens with 100mm spacing have higher energy than others.

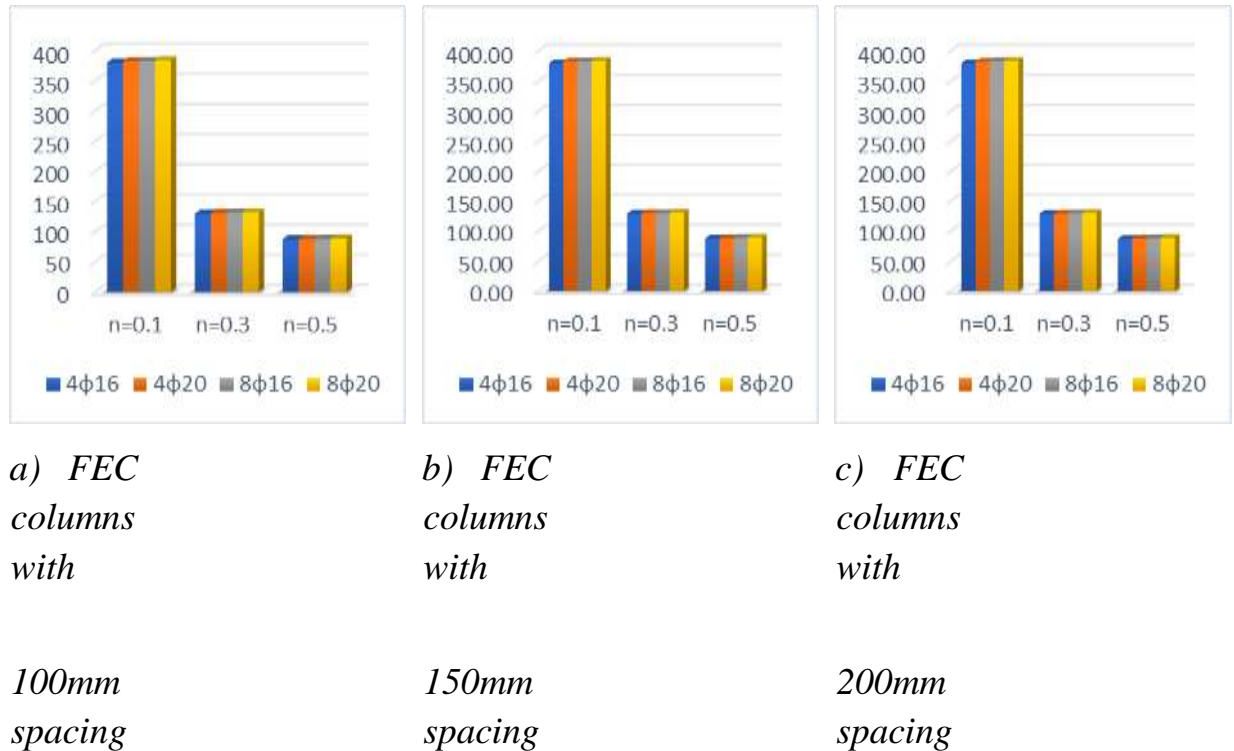


Figure 6: The cumulative energy of FEC columns.

2.4 Ductility Factor

The ductility of structural elements is used to determine their seismic behaviour and deformation capacity. The ductility factor of a specimen is defined as the ratio of the ultimate displacement to the yield displacement, with yield displacement (Δ_y) corresponding to the first yielding of the steel section and ultimate displacement (Δ_u) corresponding to the lateral displacement when the lateral load reaches the maximum load. The ductility ratio of the FEC columns was compared to several transversal bars spacing specimens in order to highlight the ductility ratio of the FEC columns as shown in Figure 7. It has been found that FEC columns with ductility of 8φ20 have the maximum ductility when compared to other FEC columns.

Specimens with a 0.1 axial load ratio have a ductility of about 3.8. Furthermore, it can be noted that the spacing between transversal bars did not have an effect on the ductility of FEC columns.

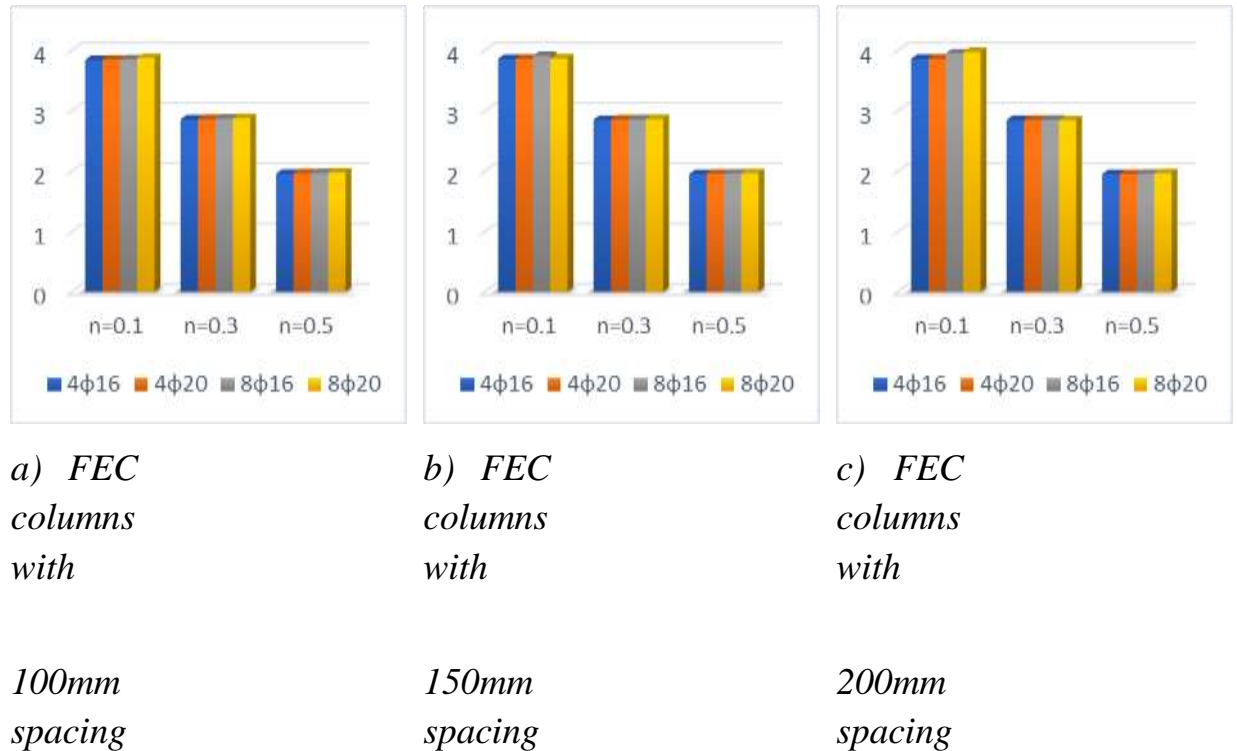


Figure 7: Ductility of FEC columns.

2.5 Stiffness initial

The main value of the rigidity of a column at the i^{th} drift has been evaluated by the following ratio (2):

$$K_i = \frac{|+P_i| + |-P_i|}{|+\Delta_i| + |-\Delta_i|}$$

(2)

where $+\Delta_i$ and $-\Delta_i$ are the peak displacements of the cycle at the i^{th} lateral displacement level in two reversal directions respectively, $+P_i$ and $-P_i$ are the loads corresponding to the peak displacements respectively, and $+P_i$ and $-P_i$ are the loads corresponding to the peak displacements respectively. Figure 8 shows that before reaching the yield displacement Δ_y , the stiffness of the specimens almost remained constant. This means the specimens are still in the elastic stage. As a result, the stiffness of the specimens decreases significantly as the curves gradually decrease until failure occurs.

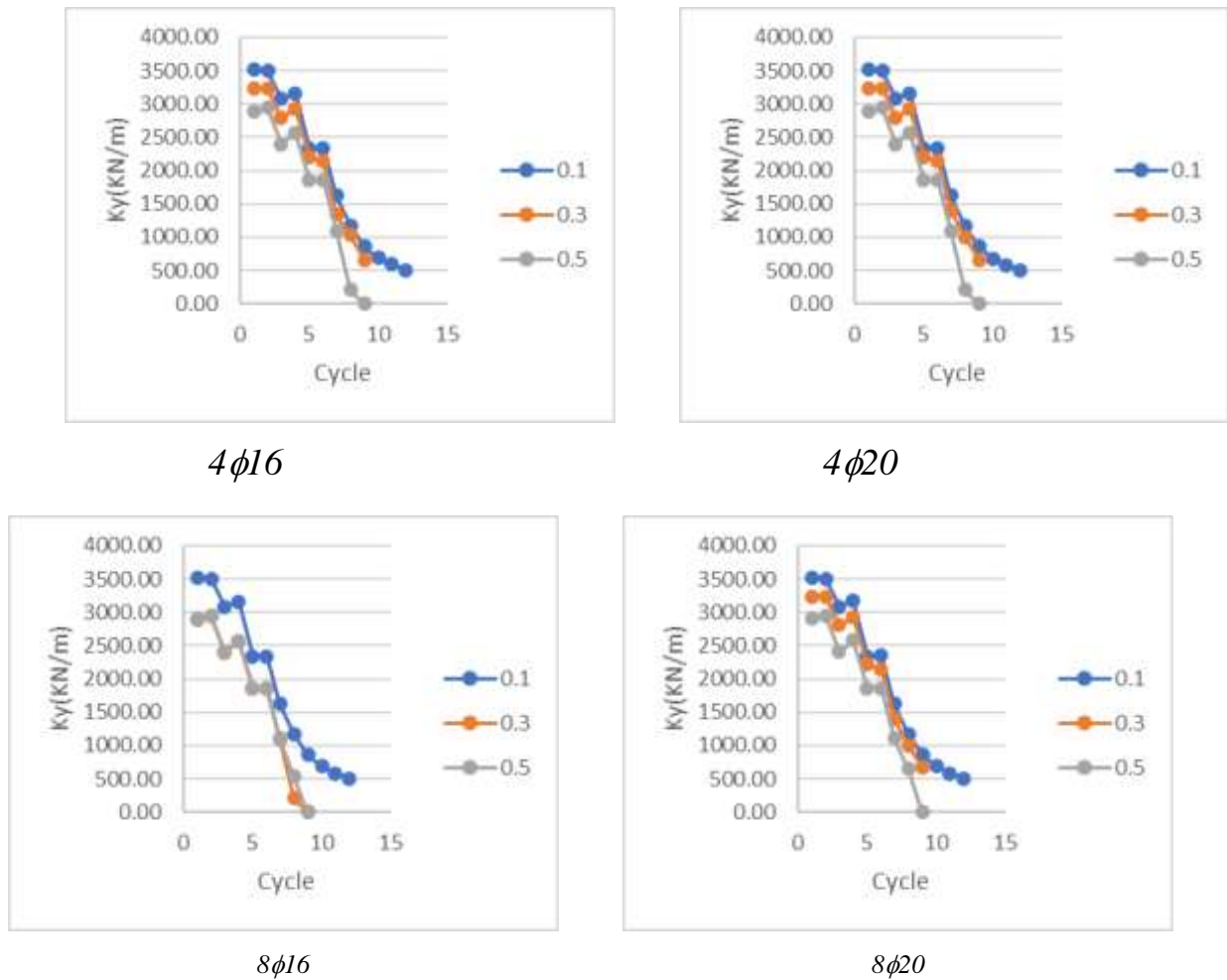


Figure 8: Influence of the axial load on the degradation of stiffness of FEC with 100 spacing.

3Conclusions

This paper investigated various parametric studies for FEC columns. The applied axial load ratio, longitudinal reinforcing bars, and transversal reinforcing bars were the main parametric variables considered in the simulation study. By comparing FEC columns with various parametric (peak load, dissipated energy, ductility factor stiffness initial and stiffness degradation) the following conclusions have been drawn:

- The longitudinal and transversal reinforcement bars have a slight effect on the FEC columns. Due to the fact that the load-bearing capacity of the steel section dominates the capacity of the reinforcing bars.

- As the longitudinal and transversal reinforcement bars ratio increases, the FEC columns become strong and rigid.
- Spacing 100mm between transversal bars attained the highest peak load, ductility, energy dissipation, higher initial stiffness and stiffness degradation much better than the others.
- Specimens with a 0.5 axial load ratio had the lowest peak load and initial stiffness, whereas the other two specimens have a peak load rise of 10.35%-27.73%, an initial stiffness increase of 50.31%-95.92%, and a ductility increase of 13.74%-15.62%.
- The axial compression ratio has a significant effect on the FEC columns.

References

1. Alkebsi, E. A. A., Ameddah, H., Outtas, T., & Almutawakel, A. (2021). Design of graded lattice structures in turbine blades using topology optimization. *International Journal of Computer Integrated Manufacturing*, 34(4), 370–384.
2. Alsamawi, A. B., Boumechra, N., & Hamdaoui, K. (2022). Numerical Parametric Study of Fully Encased Composite Columns Subjected to Cyclic Loading. *Civil Engineering Journal*, 8(01), 45–59. <https://doi.org/http://dx.doi.org/10.28991/CEJ-2022-08-01-04>
3. Alsamawi, A., & Boumechra, N. (2021). Behaviour of fully encased composite columns under cyclic loads. *Ce/Papers*, 4(2–4), 564–569. <https://doi.org/https://doi.org/10.1002/cepa.1331>
4. Aribert, M., Campiane, C., & Pacurar, V. (2003). Monotonic and cyclic behavior of fully encased Composite columns and dissipative interpretation for seismic design. *Swets&Zeitlinger B.V., Lise, The Netherlands, Proc. of STESSA 2003*, 115–122.

5. Campian, C., Nagy, Z., & Pop, M. (2015). Behavior of fully encased steel-concrete composite columns subjected to monotonic and cyclic loading. *Procedia Engineering*, 117(1), 439–451. <https://doi.org/10.1016/j.proeng.2015.08.193>
6. Chen, C., Wang, C., & Sun, H. (2014). Experimental Study on Seismic Behavior of Full Encased Steel-Concrete Composite Columns. *Journal of Structural Engineering*, 140(6), 04014024. [https://doi.org/10.1061/\(asce\)st.1943-541x.0000951](https://doi.org/10.1061/(asce)st.1943-541x.0000951)
7. Eurocode 3. (2004). *Design of steel structures Part 1-1 General rules and rules for buildings EN 1993-1-1*.
8. Eurocode 4. (2004). *Design of composite steel and concrete structures Part 1-1 General rules and rules for buildings EN 1994-1-1*.
9. Gajalakshmi, P., & Helena, H. J. (2012). Behaviour of concrete-filled steel columns subjected to lateral cyclic loading. *Journal of Constructional Steel Research*, 75, 55–63. <https://doi.org/10.1016/j.jcsr.2012.03.006>
10. Han, L. H., Huang, H., & Zhao, X. L. (2009). Analytical behaviour of concrete-filled double skin steel tubular (CFDST) beam-columns under cyclic loading. *Thin-Walled Structures*, 47(6–7), 668–680. <https://doi.org/10.1016/j.tws.2008.11.008>
11. Han, L. H., Liao, F. Y., Tao, Z., & Hong, Z. (2009). Performance of concrete filled steel tube reinforced concrete columns subjected to cyclic bending. *Journal of Constructional Steel Research*, 65(8–9), 1607–1616. <https://doi.org/10.1016/j.jcsr.2009.03.013>

12. Qian, W. W., Li, W., Han, L. H., & Zhao, X. L. (2016). Analytical behavior of concrete-encased CFST columns under cyclic lateral loading. *Journal of Constructional Steel Research*, 120, 206–220. <https://doi.org/10.1016/j.jcsr.2015.12.018>
13. Yue, J., Qian, J., & Beskos, D. E. (2019). Seismic damage performance levels for concrete encased steel columns using acoustic emission tests and finite element analysis. *Engineering Structures*, 189(March), 471–483. <https://doi.org/10.1016/j.engstruct.2019.03.077>
14. Zhu, W., Jia, J., Gao, J., & Zhang, F. (2016). Experimental study on steel reinforced high-strength concrete columns under cyclic lateral force and constant axial load. *Engineering Structures*, 125, 191–204. <https://doi.org/10.1016/j.engstruct.2016.07.018>